Structural elucidation of Cr_2O_3-Al_2O_3 catalyst: synthesis & characterization

Zulaikha Athirah Alexzman[1] and *Nur Hazirah* Rozali Annuar[1,2*]

[1]Faculty of Applied Sciences, Universiti Teknologi MARA, Cawangan Johor, Kampus Pasir Gudang, 81750 Masai, Johor, Malaysia.
[2]Advanced Biomaterials and Carbon Development, Universiti Teknologi MARA, Shah Alam, Malaysia.

Abstract. The development of active, stable, and low-cost catalysts for efficient reactions is appealing but difficult. The objectives of this study are to synthesize Cr_2O_3-Al_2O_3 catalysts and analyze their physical properties using SEM, XRD, TGA-DTA, and FTIR. The impregnation method was used to create Cr_2O_3-Al_2O_3 catalysts with five different chromium oxide loadings (3wt%, 6wt%, 9wt%, 12wt%, and 15wt%). The physical properties of the catalysts were characterized using FTIR, SEM, BET, and TGA. The FTIR spectra and SEM images of the samples confirmed that Cr_2O_3 was successfully incorporated on Al_2O_3 support. TGA was used to evaluate the weight loss and thermal stability of the catalysts during the calcination process. The hydroxyl groups of alumina, as well as its water affinity, cause more mass loss when heated because water molecules are released. The addition of chromium oxide, on the other hand, alters thermal interactions, resulting in different mass loss behavior for chromium oxide alumina. The surface area changes seen by BET analysis gave insights into the structural flexibility of the catalyst across varied loading levels. The physical properties of synthesized catalysts demonstrated their ability to be utilized in a variety of catalytic reactions.

1 Introduction

Catalysts stand as remarkable agents of transformation, serving as the dynamic agents that accelerate chemical reactions, enhance industrial processes, and reshape the contours of our technological environment [1-3]. Heterogeneous catalysts, renowned for their critical role in catalytic processes, offer a plethora of benefits that set them apart as crucial agents of conversion [4-5]. These catalysts, which operate at the phase interface, have properties that make them highly effective and versatile tools for driving chemical reactions and industrial processes. Their numerous advantages arise from their distinct composition, structural adaptability, and catalytic effectiveness, which positions them as preferred catalysts in a wide range of applications [6-7].

One of the heterogeneous catalysts is the Cr_2O_3-Al_2O_3 catalyst, which skilfully intertwines chromium oxide (Cr_2O_3) and alumina (Al_2O_3) to generate a catalytic entity of note. The Cr_2O_3-Al_2O_3 catalyst exemplifies heterogeneity by existing as a separate entity within a different phase than the reactants and products. This spatial separation has a significant benefit in that it simplifies the extraction and purification of desired products in industrial operations. Notably, the separation facilitates catalyst recycling, enabling sustainable and cost-effective operations [8-9]. In recent times, there has been growing interest in heterogeneous catalysts based on chromium oxide supported on alumina due to their distinctive redox properties, remarkable thermal stability, and versatile catalytic capabilities [10-12]. The combination of chromium oxide and alumina imparts a multitude of advantages that significantly enhance their performance in diverse catalytic applications.

Beyond its physical separation, the Cr_2O_3-Al_2O_3 catalyst has an added benefit due to its structural versatility. The composition of the catalysts can be meticulously tailored by modifying its surface properties, porosity, and active sites. This tailoring enables fine-tuning of catalytic activity, selectivity, and stability, offering precision in steering reaction outcomes. Additionally, the choice of support materials enhances these properties, granting the catalyst adaptability across diverse reaction conditions and substrates. Incorporating chromium oxide onto the alumina support results in a catalyst with exceptional thermal stability, rendering it particularly suitable for catalytic processes operating at elevated temperatures [13]. This inherent stability not only ensures prolonged catalyst activity but also maintains consistent performance over extended reaction periods. Additionally, the symbiotic interaction between chromium oxide and alumina equips the catalyst with a diverse array of acidic and basic sites, amplifying its applicability across a broad spectrum of acid-catalyzed and base-catalyzed reactions.

In light of these commendable attributes, the chromium oxide alumina catalyst emerges as a promising contender for catalytic transformations. It not

* Corresponding author: nurha8558@uitm.edu.my

only boasts inherent advantages but also holds the promise of adaptability to desired specifications. Cr_2O_3 loading provides different chemical and physical properties of the catalyst [14-15]. This claim was supported by the previous findings, which showed that the catalytic activity elevated as the Cr_2O_3 loading increased up to 8wt% Cr_2O_3 but dropped as the Cr_2O_3 loading increased to 12wt% of Cr_2O_3 [14]. In addition, Wan Isahak et al. (2017) studied the role of active chromium species via propane dehydrogenation reaction using 15wt%Cr_2O_3-Al_2O_3 and 15wt%Cr_2O_3-SiO_2 catalysts [16]. They found that the propane conversion of 15wt%Cr_2O_3-Al_2O_3 was relatively low. Therefore, this paper explores the Cr_2O_3-Al_2O_3 catalyst, covering its preparation through impregnation with different chromium oxide loading (3, 6, 9, 12 and 15wt%) and characterized using SEM, TGA, FTIR, and BET. Our study aims to understand the properties of the catalysts and examine their potential uses.

2 Experimental

2.1 Catalyst preparation

Chromium (III) nitrate nonahydrate ($Cr(NO_3)_3.9H_2O$, 99% purity) was purchased from Merck, Sdn. Bhd., Malaysia. Alumina ($C_6H_{14}O_6$, 99% purity) was acquired from R&M Chemicals, Malaysia. The technique utilized in this study was impregnation, employed to synthesize Cr_2O_3-Al_2O_3 catalysts with distinct chromium oxide (Cr_2O_3) concentrations: specifically, 3wt%, 6wt%, 9wt%, 12wt%, and 15wt%. The initial phase involved the creation of a solution containing chromium(III) nitrate nonahydrate ($Cr(NO_3)_3$. $9H_2O$). To prepare the $Cr(NO_3)_3.9H_2O$ solution, 60 g of the compound was dissolved in 500 ml of distilled water within a volumetric flask. Concurrently, 100 g of Al_2O_3 underwent calcination in a vacuum furnace under ambient air conditions at a temperature of 700 °C for a duration of one hour. Subsequently, the calcined Al_2O_3 was added to the $Cr(NO_3)_3.9H_2O$ solution and subjected to an hour-long mixing process utilizing a hot plate and a magnetic stirrer, operated consistently at 400 rpm.

To enhance homogeneity and particle dispersion within the sample, the resulting mixture underwent a ten-minute ultrasonication process. The resulting solution was subsequently dried within an oven at a temperature of 110 °C for a duration of two hours. Following this, the sample was subjected to a calcination process in an air environment at a temperature of 400 °C for a duration of three hours, rendering it ready for subsequent analysis. This sequence of steps was replicated across varying chromium oxide percentages to generate the array of catalysts under scrutiny.

2.2 Catalyst Characterization

The calcined catalysts were thermally analysed using a Perkin Elmer Thermo Gravimetric Analyzer (TGA 8000). 10 ± 0.5 mg of a sample was treated in the thermogravimetry analyser with nitrogen gas at a rate of 100 ml/min. To minimize excessive heat evolution, which could pose a safety concern and damage equipment, the sample quantity was kept minimal, around 10 mg or less. The furnace temperature was regulated between 30 and 800 °C, with a heating rate of 10 °C/min. The Bruker Fourier Transform Infrared Spectroscopy Vertex 70 (FTIR) study was performed to determine the chemical component and structure of the catalysts, as well as to investigate the primary absorption band. The analysis employs a spectral range of 600 cm^{-1} to 2200 cm^{-1}. Scanning electron micrographs (SEM, FEI Titan electron microscope) with a magnification of 1000 were used to evaluate the surface morphology of the catalysts. The porous structure of the materials was characterized by nitrogen adsorption at -196 °C using a Beckman Coulter SA3100 surface area analyser. The multipoint BET technique was used to calculate the specific surface area by linearizing the adsorption isotherm in the P/P_o range of 0 to 1. The BJH desorption method was used to create the pore size distribution function by analysing the desorption branch of the nitrogen adsorption-desorption isotherm.

3 Results and discussion

3.1 Characterization of catalysts

N_2 physisorption analysis is the most widely used technique to investigate textural properties of solid materials. Table 1 showed the surface area of all catalysts. The surface area of Al_2O_3, 3wt%Cr_2O_3-Al_2O_3, 6wt%Cr_2O_3-Al_2O_3, 9wt%Cr_2O_3-Al_2O_3, 12wt%Cr_2O_3-Al_2O_3 and 15wt%Cr_2O_3-Al_2O_3 is 148.67 cm^3/g, 143.08 cm3/g, 141.31 cm^3/g, 128.37 cm^3/g, 120.71 cm^3/g, 104.79 cm^3/g respectively. Based on the data tabulated, Al_2O_3 recorded the highest surface area compared to other catalysts. High surface area attributed to small size of the sample. Up to 12wt% of chromium loading, the surface area decreases and drastically reduced at 15wt%Cr_2O_3-Al_2O_3. The findings indicated that the deposition of chromium oxide onto the alumina support can restrict the available surface area for N_2 physisorption by obstructing pores within the material. Furthermore, increased accumulation of chromium oxide could promote the aggregation of particles, leading to a decrease in the quantity of active sites and, as a result, an expansion of the surface area.

Figure 1 showed the N_2 adsorption-desorption isotherms of the catalysts. According to the IUPAC classification, the prepared samples possessed the type IV isotherm along with a H1 hysteresis loop (narrow range of uniform mesopores where networking effects are minimal), where both are the characteristics of mesoporous materials [17] as evidenced by the corresponding pore size distribution. The adsorption branch is comprised of a region with a low slope, which is linked to multilayer adsorption on the walls of pores. Subsequently, pore condensation takes place in the mesopores, and the branch concludes with a plateau region, which signifies fully filled mesopores and minimal or absent macroporosity. The desorption

branch leads to a narrow hysteresis loop that is parallel to the adsorption branch, indicating a confined distribution of uniform mesopores and limited networking effects [18]. In the instance of adsorption isotherms, it is discovered that chromium impregnation on alumina somewhat affects the hydrogen adsorption capacity of base alumina support. The chromium-hydrogen bond is known to be more energetically weak than the alumina-hydrogen bond [19]. This could be the cause of the slight decrease in the hydrogen adsorption capacity of chromium-alumina relative to alumina that was seen in the hydrogen adsorption isotherm of chromium alumina, along with the reduction in surface area.

The presence of both chromium oxide and alumina can result in synergistic effects that significantly boost catalytic activity, surpassing what would be anticipated purely based on surface area analysis. These effects can result from intricate interactions among the various constituents of the catalyst. Although the surface area decreases as the amount of chromium oxide increases, the catalytic performance can still be enhanced or optimised through mechanisms such as improved accessibility to active sites, favourable chemical interactions, increased selectivity of the catalyst, and synergistic effects between the components of the catalyst.

Table 1. Textural properties of the Al_2O_3, 3wt%Cr_2O_3-Al_2O_3, 6wt%Cr_2O_3-Al_2O_3, 9wt%Cr_2O_3-Al_2O_3, 12wt%Cr_2O_3-Al_2O_3 and 15wt%Cr_2O_3-Al_2O_3 catalysts.

Catalysts	BET surface areas (m^2/g)
Al_2O_3	148.67
3wt% Cr_2O_3-Al_2O_3	143.08
6wt% Cr_2O_3-Al_2O_3	141.31
9wt% Cr_2O_3-Al_2O_3	128.37
12wt% Cr_2O_3-Al_2O_3	120.71
15wt% Cr_2O_3-Al_2O_3	104.79

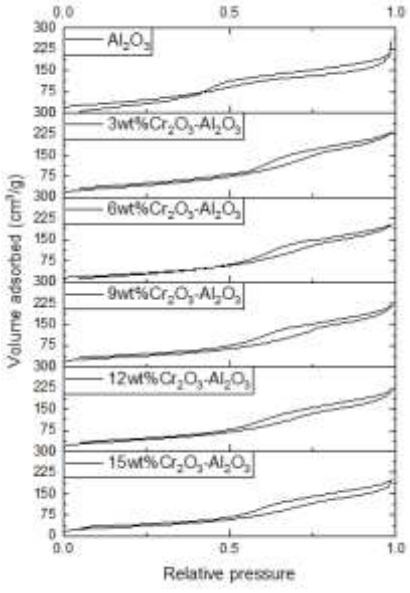

Fig. 1. Isotherm linear plot of synthesized catalysts.

Figure 2 displayed below illustrates the SEM images of Al_2O_3 and 15wt%Cr_2O_3-Al_2O_3 catalysts at 1000 magnification. The images distinctly highlighted notable distinctions in surface characteristics between both catalysts. Specifically, the difference lay in their surface features; the alumina particles exhibited an absence of minuscule chromium particles adhering to the surface. In contrast, the 15% chromium alumina showcased the presence of finely dispersed particles resembling powder (chromium) that adhere to the alumina surface. The addition of chromium oxide leads to surface modification, which is an important process for customizing surface characteristics and catalytic activity. Moreover, these particles augment the catalyst's efficacy by offering supplementary active sites for catalytic reactions, capitalizing on the well-established catalytic capabilities of chromium oxide. The extent to which chromium adhered to the surface of the alumina particles served as a critical indicator of the successful incorporation of chromium and alumina.

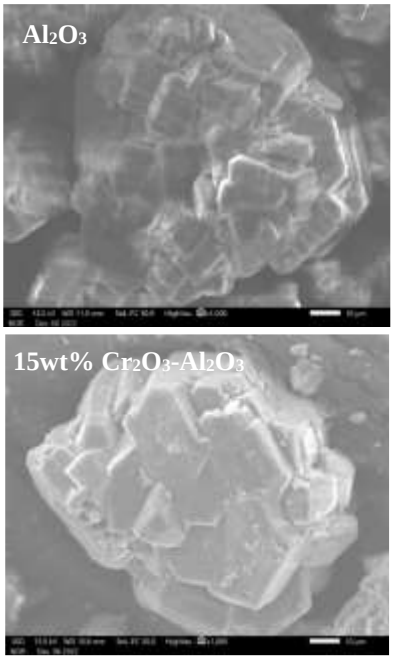

Fig. 2. SEM images of the Al_2O_3 and 15wt%Cr_2O_3-Al_2O_3 catalysts at 1000 magnification.

FTIR spectroscopy was utilised to evaluate the type of functional groups entailed in the catalysts as well as to investigate the structure variation of Al_2O_3 and varied weight percent of Cr_2O_3-Al_2O_3. Figure 3 depicted the FTIR spectra of all catalysts in the range of 600-2200 cm^{-1}. Each individual sample exhibited a distinctive peak at 690 cm^{-1}, indicative of the characteristic bending observed in Al-O-Al bonds [20]. This unequivocally signified the presence of alumina across all samples. Subsequently, a discernible peak emerged at 1052 cm^{-1}, corresponding to the bending of Al-O-H bonds [21]. However, upon meticulous scrutiny of the graph, it became evident that the intensity of each Al-O peak diminished as the chromium loadings increased, rendering the peak less conspicuous. This phenomenon can be attributed to the intricate interplay of chromium oxide.

A discernible deduction can be made that heightened percentages of chromium induce a reduction in the prominence of the peak, underscoring the effective interaction involving chromium. Thus, the increased in chromium content led to a proportional decline in the peak, thereby substantiating the successful occurrence of reactions associated with chromium. Notably, the characterization of O-H bending is observed across all samples within the spectral range of 1610 cm^{-1} [22]. This figure clearly illustrated the lack of observable chromium vibrations. This can be attributed to the challenge of precisely identifying the precise location of the chromium peak, given that it falls below 600 cm^{-1}, while the recorded results are above this threshold.

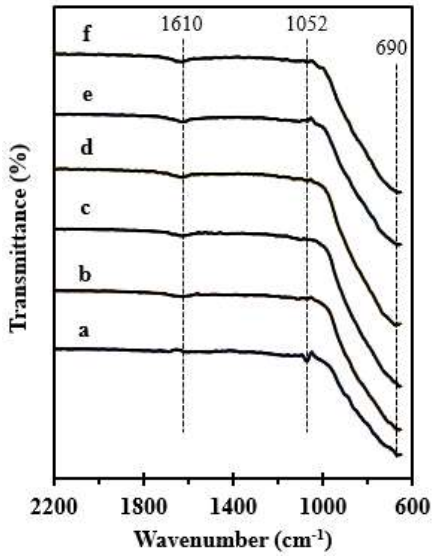

Fig. 3. FTIR spectra of (a) Al_2O_3, (b) 3wt%Cr_2O_3-Al_2O_3, (c) 6wt%Cr_2O_3-Al_2O_3, (d) 9wt%Cr_2O_3-Al_2O_3, (e) 12wt%Cr_2O_3-Al_2O_3 and (f) 15wt%Cr_2O_3-Al_2O_3 catalysts.

The weight loss and thermal stability of the samples in the calcination treatment were determined using TGA analysis. Figure 4 depicted the TGA profiles vs temperature under air conditions ranging from 30 to 800 °C. The observed TGA curve exhibited 17.6%, 3.87%, 9.62%, 9.86%, 10.4% and 11.36% total weight loss for Al_2O_3, 3wt%Cr_2O_3-Al_2O_3, 6wt%Cr_2O_3-Al_2O_3, 9wt%Cr_2O_3-Al_2O_3, 12wt%Cr_2O_3-Al_2O_3 and 15wt%Cr_2O_3-Al_2O_3 catalysts respectively. 15wt%Cr_2O_3-Al_2O_3 catalysts showed high weight loss compared to other Cr-alumina based catalyst may due to the higher mass of $Cr(NO_3)_3.9H_2O$ used during the impregnation method, which contributed to higher amount of physisorbed water in the sample. The TGA curve of all catalysts showed a gradual weight loss as temperature rises at around 30-117 °C. This is mostly due to the removal of physically adsorbed water and other volatile components from the alumina surface and pores [23]. As the temperature rose which is around 480-570 °C, the TGA curve of alumina exhibited a slight plateau or steady drop, indicating the removal of chemisorbed water and the alteration of specific hydroxyl groups on the alumina surface.

TGA analysis of chromium oxide alumina, on the other hand, showed a single weight loss occurring within the temperature range of roughly 30 °C to 100 °C. This weight loss is due to the removal of physically adsorbed water and volatile substances from the catalyst's surface and pores. The contrast in weight loss behaviour between pure alumina and chromium oxide alumina underscores the impact of the chromium oxide element on the thermal properties of the catalyst. The presence of a singular weight loss event in chromium oxide alumina predominantly pertained to the elimination of water. Conversely, pure alumina displayed two distinct weight loss events, encompassing the expulsion of water and the subsequent dehydroxylation process. The hydroxyl groups of alumina and their affinity for water contributed to its higher mass loss as it released water molecules during heating. Conversely, the introduction of chromium oxide altered the thermal interactions, resulting in a different mass loss behaviour for chromium oxide alumina. This divergence may be attributed to potential interactions between the chromium oxide species and the alumina matrix. These revelations deliver valuable insights into the thermal attributes of these materials and provide deeper comprehension of the role that chromium oxide plays in shaping the behaviour of the catalyst.

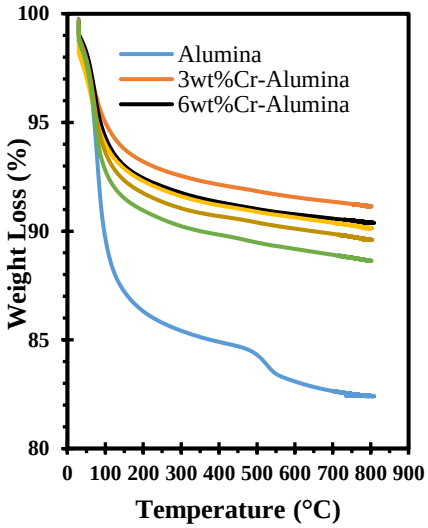

Fig. 4. TGA curves of synthesized catalysts.

4 Conclusion

The study focused on the Cr_2O_3-Al_2O_3 catalyst, examining its behaviour across different chromium oxide loading levels (3wt% to 15wt%). This methodological approach yielded a nuanced understanding of how distinct levels of chromium oxide loading influenced both the physical characteristics of the catalyst, including surface area and thermal stability, and the intricate dynamics of the interaction between chromium and alumina. The shifts in surface areas, observed through BET analysis, provided insights into the structural adaptability of the catalyst across varying loading levels. The mesoporous nature, evident from type IV isotherms, connected loading to textural properties. Observable alterations in thermal behaviour,

as indicated by TGA findings, shed light on how the presence of chromium oxide contributed to the stability and thermal profile of the catalyst. Furthermore, the discernible shifts in Al-O bending peaks revealed by FTIR analysis highlighted the interaction between chromium and alumina, showcasing its distinct variation with different chromium oxide loadings. SEM images visually confirmed successful incorporation of chromia. This multi-technique analysis deepened our understanding of how chromium oxide loading intricately influences the Cr_2O_3-Al_2O_3 catalyst, enhancing its potential applications.

This work was supported by Geran Penyelidikan Bestari Phase 2/2021 (600-TNCPI 5/3/DDN (01) (022/2021)) from Universiti Teknologi MARA, Cawangan Johor. We thank School of Chemical Engineering, College of Engineering, Universiti Teknologi MARA, Johor Branch, Pasir Gudang Campus, Malaysia for the access to the instrumentations and facilities.

References

1. H. Shahbeik, W. Peng, H.K.S. Panahi, M. Dehhaghi, G.J. Guillemin, A. Fallahi, H. Amiri, M. Rehan, D. Raikwar, H. Latine, B. Pandalone, B. Khoshnevisan, C. Sonne, L Vaccaro, A.S Nizami, V.K. Gupta, S.S. Lam, J. Pan, R. Luque, B. Sels, M. Tabatabaei, M. Aghbashlo, Synthesis of liquid biofuels from biomass by hydrothermal gasification: A critical review. Renew. Sust. Energ. Rev. **167**, 112833 (2022)
2. Z. Khan, F. Javed, Z. Shamair, A. Hafeez, T. Fazal, A. Aslam, W.B. Zimmerman, F. Rehman, Current developments in esterification reaction: A review on process and parameters. J. Ind. Eng. Chem. **103**, 80 (2021)
3. E.C. Gaudino, G. Cravotto, M. Manzoli, S. Tabasso, Sono-and mechanochemical technologies in the catalytic conversion of biomass. Chem. Soc. Rev. **50**, 1785 (2021)
4. D.P. Debecker, S.L. Bras, C. Boissière, A. Chaumonnotc, C. Sanchez, Aerosol processing: a wind of innovation in the field of advanced heterogeneous catalysts. Chem. Soc. Rev. **47**, 4112 (2018)
5. P. Sudarsanam, R. Zhong, S.V. den Bosch, S.M. Coman, V.I. Parvulescu, B.F. Sels, Functionalised heterogeneous catalysts for sustainable biomass valorisation. Chem. Soc. Rev. **47**, 8349 (2018)
6. M.Y. Masoomi, A. Morsali, A. Dhakshinamoorthy, H. Garcia, Mixed-metal MOFs: unique opportunities in metal–organic framework (MOF) functionality and design. Angew. Chem. **131**, 15330 (2019)
7. N. Muhd Julkapli, S. Bagheri, Graphene supported heterogeneous catalysts: An overview. Int. J. Hydrogen Energy **40**, 948 (2015)
8. X. Wang, T. Saba, H.H.P. Yiu, R.F. Howe, J.A. Anderson, Cofactor *NAD (P)* H regeneration inspired by heterogeneous pathway. J. Shi. Chem. **2**, 621 (2017)
9. S.H.Y. Sayid Abdullah, N.H. Mohamad Hanapi, A. Azid, R. Umar, H. Juahir, H. Khatoon, A. Endut, A review of biomass-derived heterogeneous catalyst for a sustainable biodiesel production. Renew. Sust. Energ. Rev. **70**, 1040 (2017)
10. G. Wang, N. Song, K. Lu, W. Wang, L. Bing, Q. Zhang, H. Fu, F. Wang, D. Han, Ca-doped CrO_X/γ-Al_2O_3 catalysts with improved dehydrogenation performance for the conversion of isobutane to isobutene. Catal. **9**, 968 (2019)
11. Y. Wang, J. Yang, R. Gu, L. Peng, X. Guo, N. Xue, Y. Zhu, W. Ding, Crystal-facet effect of γ-Al_2O_3 on supporting CrO_x for catalytic semihydrogenation of acetylene ACS Catal. **8**, 6419 (2018)
12. V.Z. Fridman, X. Rong, Investigating the CrO_x/Al_2O_3 dehydrogenation catalyst model: II. Relative activity of the chromium species on the catalyst surface. Appl. Catal. A: Gen. **530**, 154 (2017)
13. A. Węgrzyniak, S. Jarczewski, A. Węgrzynowicz, B. Michorczyk, P. Kuśtrowski, P. Michorczyk, Catalytic behavior of chromium oxide supported on nanocasting-prepared mesoporous alumina in dehydrogenation of propane. J. Nanomater. **7**, 249 (2017)
14. N.H.R. Annuar, L.P. Teh, H.D. Setiabudi, M.A.A. Aziz, N.M. Salam A.A. Jalil, The study of chromium oxide loading on platinum chromium oxide zirconia catalyst for n-dodecane and 1, 4-diisopropylbenzene hydrocracking, IOP Conf. Ser. Mater. Sci. Eng. **736**, 042039 (2020)
15. Z.A. Alexzman, N.H.R. Annuar, N. Salamun, S.N.H.M. Yusoff, A.R.M. Daud, Chromium oxide silica catalyst: Synthesis and characterization, Mater. Today: Proc. **57**, 1301- (2022)
16. W.N.R. Wan Isahak, Z.A.C. Ramli, M.W. Mohamed Hisham, M.A. Yarmo, Magnesium oxide nanoparticles on green activated carbon as efficient CO_2 adsorbent, Malaysian J. Anal. Sci. **21**, 119 (2017)
17. J. Chen, H. Zou, O. Yao, M. Luo, X. Li, Z.H. Lu, Cr_2O_3-modified NiFe nanoparticles as a noble-metal-catalyst for complete dehydrogenation of hydrazine in aqueous solution. Appl. Surf. Sci. **501**, 144247 (2020)
18. F.J. Sotomayor, K.A. Cychosz, M. Thommes, Characterization of micro/mesoporous materials by physisorption: concepts and case studies. Acc. Mater. Surf. Res. **3**, 34 (2018)
19. D.Y. Gaikwad, D. Bandyopadhyay, S. Prabhu, S. Mohan, S. Mishra, An insight into hydrogen isotopic separation on iron-alumina and chromium-alumina as stationary phase in gas

chromatographic method. Int. J. Hydrogen Energy **42**, 15557 (2017)

20. J. Roy, N. Bandyopadhyay, S. Das, S. Maitra, Studies on the formation of mullite from diphasic Al_2O_3-SiO_2 gel by fourier transform infrared spectroscopy. Iran. J. Chem. Chem. Eng. **30**, 65 (2011)
21. J.T. Anandhi, S.L. Rayer, T. Chithambarathanu, Synthesis, FTIR studies and optical properties of aluminium doped chromium oxide nanoparticles by microwave irradiation at different concentrations. Chem. Mater. Eng. **5**, 43 (2017)
22. M. Mahinroosta, A. Allahverdi, Production of nanostructured γ-alumina from aluminum foundry tailing for catalytic applications. Int. Nano Lett. **8**, 255 (2018)
23. Y.F. Adans, A.R. Martins, R.E. Coelho, C.F. das Virgens, A.D. Ballarinid, L.S. Carvalhoa, A simple way to produce γ-alumina from aluminum cans by precipitation reactions. Mat. Res. **19**, 977 (2016)